N-Linked Neutral Sugar Chains of Aminopeptidase N Purified from Rat Small Intestinal Brush-Border Membrane†

Seiichi Takasaki,‡ Roger H. Erickson,§ Young S. Kim,§ Naohisa Kochibe,∥ and Akira Kobata*,‡

Department of Biochemistry, Institute of Medical Science, University of Tokyo, Minato-ku, Tokyo 108, Japan, Gastrointestinal Research Laboratory (151-M2), Veterans Administration Medical Center, 4150 Clement Street, San Francisco, California 94121, Department of Medicine, University of California, San Francisco, California 94143, and Department of Biology, Faculty of Education, Gunma University, Maebashi 371, Japan

Received December 11, 1990; Revised Manuscript Received June 26, 1991

ABSTRACT: Neutral oligosaccharides, which accounted for 74% of the total N-linked sugar chains released by hydrazinolysis of rat small intestinal aminopeptidase N, were investigated on a structural basis. They are mainly composed of complex-type sugar chains with tri- and tetraantennary structures, and small amounts of high mannose type sugar chains (7% of the total neutral sugar chains) are also included. The unique feature of the complex-type sugar chains is that most of them contain terminal *N*-acetylglucosamine residues and blood group H antigenic determinants in their outer chain moieties, and bisecting *N*-acetylglucosamine residues in their trimannosyl cores. Both the type 1H and type 2H determinants are found, but the former is mainly expressed at the distal portions of the outer chain moieties of the oligosaccharides.

Brush-border membrane of mammalian small intestine contains a variety of enzymes that play essential roles in the hydrolysis of ingested dietary nutrients. These enzymes are synthesized in polarized epithelial cells of the small intestine and are then transported to the apical membrane domain by a still unknown mechanism. With a consideration of the current work on the subcellular localization of lysosomal enzymes, it is tempting to postulate the possibility that the sugar moiety may serve as a traffic signal to transport the intestinal membrane glycoproteins to the apical surface or the basolateral surface. One of the approaches to investigate this problem is to elucidate the structures of the sugar chains of apical and basolateral membrane glycoproteins.

Aminopeptidase N (EC 3.4.11.2), which occurs in the apical surface, has been purified from the mucosa of rat small intestine (Kim & Brophy, 1976). The enzyme contains 20% sugar by weight, and the data of its sugar composition analysis indicated that N-linked sugar chains are included in the enzyme. From the interaction of the enzyme with some lectin–Sepharose columns (Erickson & Kim, 1983), it has been suggested that the enzyme is composed of several molecules with different sets of sugar chains. Kinetic analysis of these enzyme molecules also revealed some differences. To be noted is that in spite of the high sugar content 70% of the enzyme does not interact with any of the Con A[1]–, RCA-I– and WGA–Sepharose columns, suggesting that unusual derivatizations at sugar chains are included in the enzyme as major components. The behavior in immobilized lectin columns has also been shown to differ between the enzymes in the proximal and in the distal segments of small intestine (Morita et al., 1986).

Accordingly, the detailed structural analysis of these sugar chains has become an important step to understand the basis of the heterogeneous nature of the enzyme and to find a clue to the possible role of the sugar moiety in the specific transport of the enzyme to the apical surface. In this paper, we will describe the structures of major N-linked, neutral sugar chains of rat small intestinal aminopeptidase N.

Materials and Methods

Chemicals, Enzymes, and Lectins. NaB^3H_4 (319 mCi/mmol) and NaB^2H_4 were purchased from New England Nuclear, Boston, MA, and from Merck Co., Darmstadt, FRG, respectively. β-Galactosidase, α-mannosidase, and β-*N*-acetylhexosaminidase were purified from jack bean meal as described by Li and Li (1972), and β-galactosidase and β-*N*-acetylhexosaminidase were also purified from the culture fluid of *Diplococcus pneumoniae* according to the method of Glasgow et al. (1977). *Aspergillus saitoi* α-mannosidases I (Ichishima et al., 1981) and II (Amano & Kobata, 1986) were purified according to the cited references. α-L-Fucosidase from *Corynebacterium sp.* was kindly provided by Takara Shuzo Co. Ltd., Ohtsu, Japan. Oligosaccharides were incubated with α-fucosidase (2.5 units) in 50 μL of 0.1 M phosphate buffer, pH 8.2, overnight. Under this condition, the enzyme acts on the Fucα1→2Gal linkage but not on the Fucα1→3 and 4GlcNAc linkages and the Fucα1→6GlcNAc linkage. Other glycosidase digestions were performed as previously described (Yoshima et al., 1980).

Chromatography on an *Aleuria aurantia* lectin (AAL)–Sepharose (Yamashita et al., 1985), concanavalin A (Con A)–Sepharose (Ogata et al., 1975), or *Ricinus communis* agglutinin I (RCA-I)–Sepharose (Kornfeld et al., 1981) column was performed according to the cited references. Aminopeptidase N was purified from rat small intestine as described previously (Kim & Brophy, 1976), and the enzyme that had been designated "peptidase F" was used in this study.

† This work was supported by a Grant-in-Aid for Scientific Research from the Ministry of Education, Science, and Culture of Japan, by Grant AM17938 from the National Institute of Health, and by the Veterans Administration Medical Research Service.

* To whom correspondence should be addressed.

‡ University of Tokyo.

§ Veterans Administration Medical Center and University of California.

∥ Gunma University.

[1] Abbreviations: Con A, concanavalin A; RCA, *Ricinus communis* agglutinin; WGA, wheat germ agglutinin; AAL, *Aleuria aurantia* lectin.

0006-2960/91/0430-9102$02.50/0

Liberation of the N-Linked Sugar Chains from Aminopeptidase N as Oligosaccharides. The purified aminopeptidase N (3 mg) was subjected to hydrazinolysis as previously described (Takasaki et al., 1982). One-fourth of the oligosaccharide fraction thus obtained was reduced with NaB^3H_4 after the addition of 10 nmol of xylose as an internal standard. By comparison of the radioactivities incorporated into the oligosaccharide fraction and xylose that were separated by paper chromatography, the amount of sugar chains was calculated to be 20.4 mol in 1 mol of a dimeric form of aminopeptidase N. The molecular weight of this dimeric form was reported to be 280000 (Kim & Brophy, 1976).

The remaining oligosaccharide fraction was reduced with NaB^2H_4 to obtain the sample for methylation analysis. For the ease of detection of the deuterium-labeled oligosaccharides in further fractionation procedures, one-tenth of the tritium-labeled oligosaccharide mixture was added to this deuterium-labeled oligosaccharide fraction.

Analytical Methods. Paper electrophoresis was performed by using pyridine/acetate buffer, pH 5.4 (pyridine/acetic acid/water 3:1:387) at a potential of 73 V/cm for 3 h. Bio-Gel P-4 column chromatography (Yamashita et al., 1982) and methylation analysis (Kagawa et al., 1988) were carried out as described in the cited references. Smith degradation was carried out basically according to the previous procedure (Takasaki et al., 1984) with the minor modification that acid hydrolysis was performed for 2 h.

Oligosaccharides. Mono-, di-, and trisialyl derivatives of Galβ1→4GlcNAcβ1→2Manα1→6[Galβ1→4GlcNAcβ1→4-(Galβ1→4GlcNAcβ1→2)Manα1→3]Manβ1→4GlcNAc-β1→4$GlcNAc_{OT}$[2] (Gal_3·$GlcNAc_3$·Man_3·GlcNAc·$GlcNAc_{OT}$) were prepared from fetuin by hydrazinolysis (Takasaki & Kobata, 1986). GlcNAcβ1→6(GlcNAcβ1→2)Manα1→6-(GlcNAcβ1→4)[GlcNAcβ1→4(GlcNAcβ1→2)Manα1→3]-Manβ1→4 GlcNAcβ1→4(Fucα1→6)$GlcNAc_{OT}$ (bisected $GlcNAc_4$·Man_2·GlcNAc·Man·GlcNAc·Fuc·$GlcNAc_{OT}$) and GlcNAcβ1→2Manα1→6(GlcNAcβ1→4)[GlcNAcβ1→4-(GlcNAcβ1→2)Manα1→3]Manβ1→4GlcNAcβ1→4-(Fucα1→6)$GlcNAc_{OT}$ (bisected $GlcNAc_3$·Man_2·GlcNAc·Man·GlcNAc·Fuc·$GlcNAc_{OT}$) were obtained from bovine kidney γ-glutamyltranspeptidase as described in a previous paper (Yamashita et al., 1983d). GlcNAcβ1→6-(GlcNAcβ1→2)Manα1→6[GlcNAcβ1→4(GlcNAcβ1→2)-Manα1→3]Manβ1→4GlcNAcβ1→4(Fucα1→6)$GlcNAc_{OT}$ ($GlcNAc_4$·Man_3·GlcNAc·Fuc·$GlcNAc_{OT}$) and GlcNAcβ1→-2Manα1→6[GlcNAcβ1→4(GlcNAcβ1→2)Manα1→3]-Manβ1→4GlcNAcβ1→4 (Fucα1→6)$GlcNAc_{OT}$ ($GlcNAc_3$·Man_3·GlcNAc·Fuc·$GlcNAc_{OT}$) were prepared from recombinant human erythropoietin as previously described (Takeuchi et al., 1988). Manα1→6(Manα1→3)Manβ1→-4GlcNAcβ1→4(Fucα1→6)$GlcNAc_{OT}$ (Man_3·GlcNAc·Fuc·$GlcNAc_{OT}$) was prepared by jack bean β-*N*-acetylhexosaminidase digestion of $GlcNAc_4$·Man_3·GlcNAc·Fuc·$GlcNAc_{OT}$. Manα1→6(Manα1→3)Manβ1→4GlcNAcβ1→-4$GlcNAc_{OT}$ (Man_3·GlcNAc·$GlcNAc_{OT}$) was also prepared by digestion of Gal_3·$GlcNAc_3$·Man_3·GlcNAc·$GlcNAc_{OT}$ with a mixture of jack bean β-galactosidase and jack bean β-*N*-acetylhexosaminidase. Manα1→3Manβ1→4GlcNAcβ1→-4$GlcNAc_{OT}$ (Man_2·GlcNAc·$GlcNAc_{OT}$) and Manβ1→-4GlcNAcβ1→4$XylNAc_{OT}$ (Man·GlcNAc·$XylNAc_{OT}$) were prepared by one cycle and two cycles of Smith degradations of $GlcNA_3$·Man_3·GlcNAc·Fuc·$GlcNAc_{OT}$, respectively.

[2] Subscript OT indicates NaB^3H_4-reduced oligosaccharides. All sugars mentioned in this paper have the D-configuration except for fucose, which has the L-configuration.

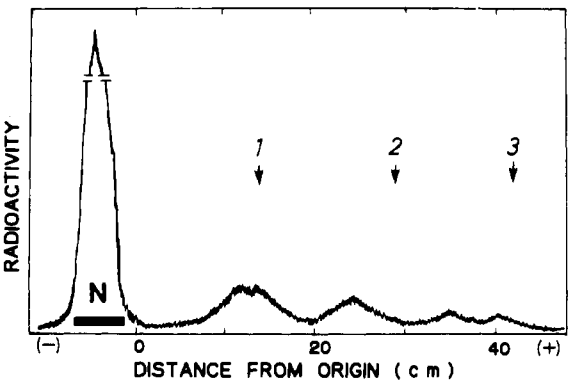

FIGURE 1: Separation of neutral and acidic oligosaccharides obtained from rat small intestinal aminopeptidase N. The oligosaccharide fraction released by hydrazinolysis was subjected to high-voltage paper electrophoresis at pH 5.4. The arrows 1, 2, and 3 indicate the positions of authentic mono-, di-, and trisialylated Gal_3·$GlcNAc_3$·Man_3·GlcNAc·$GlcNAc_{OT}$, respectively.

RESULTS

Paper Electrophoresis of Oligosaccharides from Rat Intestinal Aminopeptidase N and Preliminary Analysis of the Major Neutral Oligosaccharides. The radioactive oligosaccharide mixture released from aminopeptidase N by hydrazinolysis was subjected to high-voltage paper electrophoresis at pH 5.4. As shown in Figure 1, a neutral oligosaccharide fraction (N), which amounted to 74% of the total oligosaccharides, and at least four acidic oligosaccharide fractions were separated. When a portion of fraction N was applied to a Con A–Sepharose column, 93% of the oligosaccharides were passed through and others were bound to the column. Preliminary analysis of the major oligosaccharides recovered in the Con A unbound fraction by Bio-Gel P-4 column chromatography showed a very complicated elution pattern, suggesting that more than 10 components are included (data not shown). However, sequential exoglycosidase digestion with *Corynebacterium* α-fucosidase, jack bean β-galactosidase, and jack bean β-*N*-acetylhexosaminidase converted all the multiple components in this fraction to two radioactive components corresponding to fucosylated and non-fucosylated trimannosyl cores, Man_3·GlcNAc·Fuc·$GlcNAc_{OT}$ and Man_3·GlcNAc·$GlcNAc_{OT}$, respectively. When the prior digestion with α-fucosidase was omitted, conversion to the trimannosyl cores was no more than 10% of fraction N. These results suggest that the major neutral oligosaccharides recovered in the Con A unbound fraction are of complex type and their outer chain moieties are extensively fucosylated. It is also suggested that oligosaccharides with *N*-acetyllactosamine repeating units are not included in this fraction, since this type of oligosaccharide, if present, should not be converted to the trimannosyl cores by sequential glycosidase digestion with α-fucosidase, β-galactosidase, and β-*N*-acetylhexosaminidase. These structural aspects of oligosaccharides were examined in detail after fractionation of oligosaccharides as described below.

Fractionation of Neutral Oligosaccharides by Serial Lectin Column Chromatography and Bio-Gel P-4 Column Chromatography. Due to the heterogeneous nature of fraction N, it was fractionated by serial lectin column chromatography. As shown in Figure 2, fraction N was first applied to an AAL–Sepharose column. The unbound fraction and the bound fraction, which was eluted from the column by the buffer containing 1 mM fucose, were separately applied to Con A–Sepharose columns. Most of the AAL-unbound fraction was passed through the column, and the remainder was eluted from the column by the buffer containing 0.1 M methyl α-

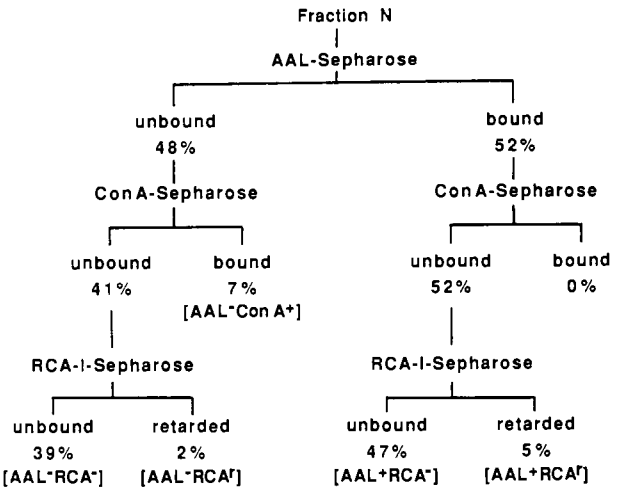

FIGURE 2: Fractionation of neutral oligosaccharides by serial lectin column chromatography. Numbers indicate the percent molar ratios of each fraction to the total neutral oligosaccharides.

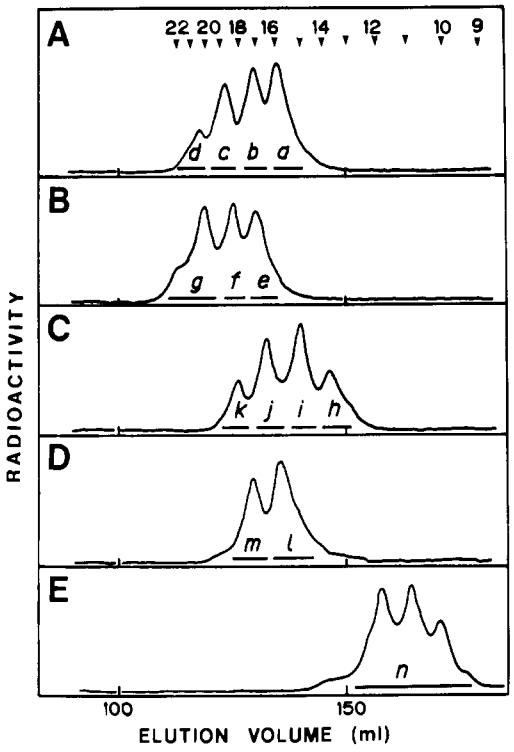

FIGURE 3: Bio-Gel P-4 column chromatography of the neutral oligosaccharides fractionated by lectin columns: (panel A) the AAL^+RCA^- fraction; (panel B) the AAL^+RCA^r fraction; (panel C) the AAL^-RCA^- fraction; (panel D) the AAL^-RCA^r fraction; (panel E) the $AAL^-Con\ A^+$ fraction. Black arrowheads indicate the elution positions of glucose oligomers, and numbers indicate the glucose units.

mannoside ($AAl^-Con\ A^+$). In contrast, all the AAL-bound fraction was recovered in the Con A unbound fraction. Both Con A unbound fractions were finally separated into the unbound (AAL^-RCA^- and AAL^+RCA^-) and the retarded (AAL^-RCA^r and AAL^+RCA^r) fractions by RCA-I–Sepharose column chromatography. The distribution of the oligosaccharides in each fraction is summarized in Figure 2. The sum total of the RCA^- fractions accounted for 86% of the total neutral oligosaccharides. This seems to be consistent with the preliminary data described above that major oligosaccharides are of complex type with extensively fucosylated outer chains.

Each of the five fractions thus obtained was then applied to a column of Bio-Gel P-4. As shown in Figure 3, the AAL^+RCA^- (panel A), the AAL^+RCA^r (panel B), the AAL^-RCA^- (panel C), the AAL^-RCA^r (panel D), and the $AAL^-Con\ A^+$ (panel E) fractions were separated into several components. These components were designated a to n as indicated in the figure and were subjected to detailed structural analysis.

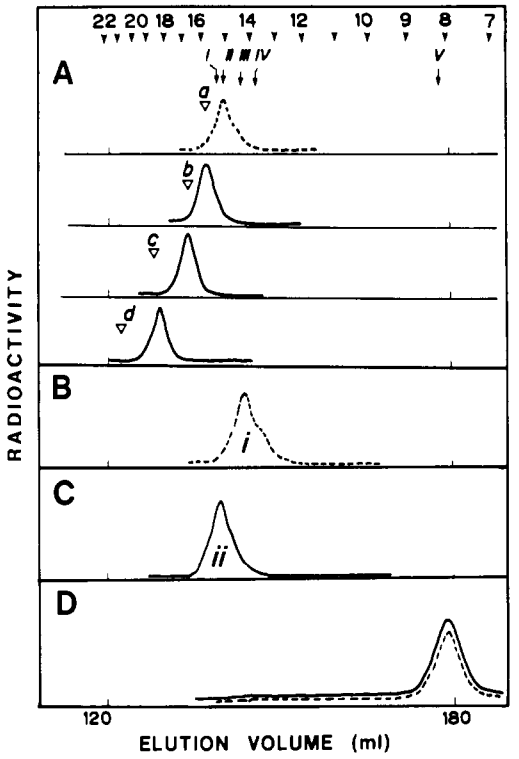

FIGURE 4: Sequential exoglycosidase digestion of components a, b, c, and d. The components a, b, c, and d, the original elution positions of which were indicated by open triangles, were digested with *Corynebacterium* α-fucosidase (panel A). The defucosylated component a (dotted line in panel A) was sequentially digested with jack bean β-galactosidase (panel B) and jack bean β-*N*-acetylhexosaminidase (dotted line in panel D). The defucosylated components b, c, and d (solid lines in panel A) were all converted to the same radioactive products by sequential digestion with jack bean β-galactosidase (panel C) and jack bean β-*N*-acetylhexosaminidase (solid line in panel D). Arrows indicate the elution positions of authentic oligosaccharides: I, bisected $GlcNAc_4$·Man_2·GlcNAc·Man·GlcNAc·Fuc·$GlcNAc_{OT}$; II, $GlcNAc_4$·Man_3·GlcNAc·Fuc·$GlcNAc_{OT}$; III, bisected $GlcNAc_3$·Man_2·GlcNAc·Man·GlcNAc·Fuc·$GlcNAc_{OT}$; IV, $GlcNAc_3$·Man_3·GlcNAc·Fuc·$GlcNAc_{OT}$; and V, Man_3·GlcNAc·Fuc·$GlcNAc_{OT}$. The black arrowheads are the same as in Figure 3.

Structural Analysis of Oligosaccharides in the AAL^+RCA^- Fraction. Elution positions of components a, b, c, and d upon Bio-Gel P-4 column chromatography did not change after incubation with jack bean β-galactosidase. When these components were incubated with *Corynebacterium* α-fucosidase, one fucose residue was removed each from components a and b, two from component c, and three from component d (Figure 4A). α-Fucosidase used here specifically cleaves the Fucα1→2Gal linkage. Occurrence of this fucosyl linkage in these components was confirmed by methylation analysis showing that 3,4,6-tri-*O*-methylgalactitol detected in the AAL^+RCA^- fraction vanishes after α-fucosidase digestion with an appearance of 2,3,4,6-tetra-*O*-methylgalactitol (Table I). In consistent with no release of galactose residue from component a–d by β-galactosidase digestion, the methylation data also indicate the absence of 2,3,4,6-tetra-*O*-methylgalactitol in the AAL^+RCA^- fraction. The following jack bean β-galactosidase digestion of the defucosylated component a in Figure 4A (dotted line) removed one galactose residue, and the resulting radioactive product was eluted as a peak with a shoulder (named peak i) at the positions of bisected

Table I: Methylation Analysis of Oligosaccharides Included in the AAL$^+$RCA$^-$ Fraction

methylated sugars	molar ratio[a]				
	α-fucosidase		peaks[d]		
	−[b]	+[c]	i	ii	i + ii[e]
fucitol					
2,3,4-tri-*O*-Me	2.2	0.9	0.8	0.9	0.9
galacititol					
2,3,4,6-tetra-*O*-Me	0	1.4	0	0	0
3,4,6-tri-*O*-Me	1.3	0	0	0	0
mannitol					
3,4,6-tri-*O*-Me	0.4	0.4	1.0	0	0.4
3,6-di-*O*-Me	0.9	0.9	0.9	0.9	0.9
3,4-di-*O*-Me	0.5	0.5	0	0.8	0.5
2,4-di-*O*-Me	0.2	0.2	0.2	0.2	0.2
2-mono-*O*-Me	0.8	0.8	0.8	0.8	0.8
2-*N*-methylacetamido-2-deoxyglucitol					
1,3,5-tri-*O*-Me	0.8	0.9	0.9	0.8	0.8
3,4,6-tri-*O*-Me	2.8	2.7	3.4	4.3	4.0
3,6-di-*O*-Me	1.4	1.3	0.9	0.9	0.9
4,6-di-*O*-Me	1.0	0.9	0	0	0

[a] Expressed by taking the value of 2,4-di- and 2-mono-*O*-methylmannitols as 1.0. [b] Intact AAL$^+$RCA$^-$ fraction. [c] The AAL$^+$RCA$^-$ fraction digested with *Corynebacterium* α-fucosidase. [d] Obtained by jack bean β-galactosidase digestion (see Figure 4B,C). [e] Calculated from the experimental values of peaks i and ii on the basis that the molar ratio of peaks i and ii is 0.38:0.62.

$GlcNAc_3{\cdot}Man_2{\cdot}GlcNAc{\cdot}Man{\cdot}GlcNAc{\cdot}Fuc{\cdot}GlcNAc_{OT}$ and $GlcNAc_3{\cdot}Man_3{\cdot}GlcNAc{\cdot}Fuc{\cdot}GlcNAc_{OT}$ (Figure 4B). On the other hand, jack bean β-galactosidase digestion removed one, two, and three galactose residues from the defucosylated components *b*, *c*, and *d* in Figure 4A (solid lines), respectively, and all the radioactive products from these components were eluted as a slightly broad peak (named peak ii) at the positions of bisected $GlcNAc_4{\cdot}Man_2{\cdot}GlcNAc{\cdot}Man{\cdot}GlcNAc{\cdot}Fuc{\cdot}GlcNAc_{OT}$ and $GlcNAc_4{\cdot}Man_3{\cdot}GlcNAc{\cdot}Fuc{\cdot}GlcNAc_{OT}$ (Figure 4C). These results indicate that component a has one Fucα1→2Galβ1→ group linked to peak i and that components b, c, and d have one, two, and three Fucα1→2Galβ1→ groups linked to peak ii, respectively.

By jack bean β-*N*-acetylhexosaminidase digestion, peak i was converted to a fucosylated trimannosyl core, $Man_3{\cdot}GlcNAc{\cdot}Fuc{\cdot}GlcNAc_{OT}$, with release of four *N*-acetylglucosamine residues from the peak and three residues from the shoulder (Figure 4D, dotted line). Methylation analysis of peak i indicated the occurrence of 2-mono-*O*-methyl and 2,4-di-*O*-methylmannitols in a molar ratio of 4:1, suggesting that bisected and non-bisected oligosaccharides are included (Table I). Therefore, peak i is supposed to have the structures

i-A

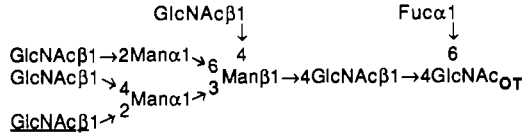

i-B

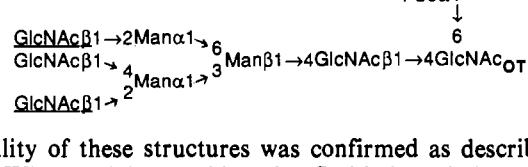

Reliability of these structures was confirmed as described below. When peak i was subjected to Smith degradation, only one radioactive product corresponding to Manα1→3Manβ1→4GlcNAcβ1→4GlcNAc$_{OT}$ was obtained (Figure 5A). This product was then converted to Manβ1→4GlcNAcβ1→4XylNAc$_{OT}$ by another cycle of Smith degradation (Figure 5B). These results indicate that the

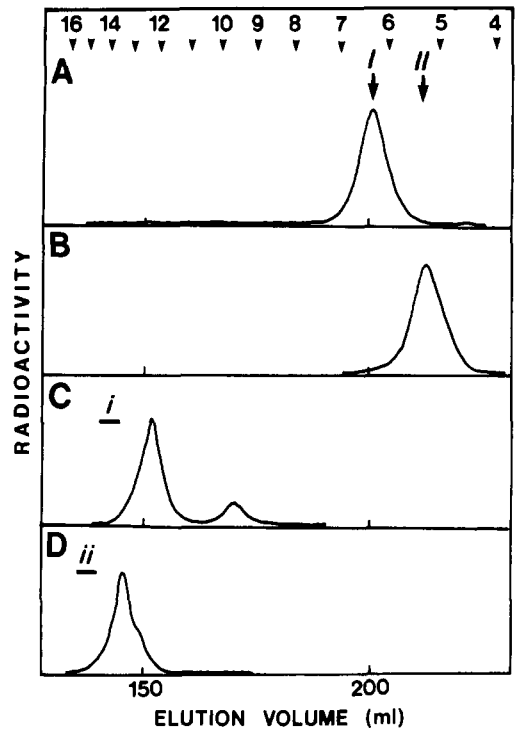

FIGURE 5: Smith degradation and diplococcal β-*N*-acetylhexosaminidase digestion of peaks i and ii. Peak i in Figure 4 was subjected to one cycle (panel A) and two cycles (pane B) of Smith degradation, and the same results were obtained with peak ii. Peaks i (panel C) and ii (panel D), the original elution positions of which were indicated by bars, were digested with diplococcal β-*N*-acetylhexosaminidase. Arrows indicate the elution positions of authentic oligosaccharides; I, $Man_2{\cdot}GlcNAc{\cdot}GlcNAc_{OT}$; II, $Man{\cdot}GlcNAc{\cdot}XylNAc_{OT}$. The black arrowheads and numbers are the same as in Figure 3.

GlcNAcβ1→4(GlcNAcβ1→2)Manα1→ group is exclusively linked at the C-3 position of the β-mannosyl residue of fucosylated trimannosyl core. It is well-known that the *N*-acetylglucosamine residues underlined in the proposed structures can be removed by incubation with diplococcal β-*N*-acetylhexosaminidase according to its strict substrate specificity (Yamashita et al., 1981). When peak i was incubated with this enzyme, it was converted to two expected radioactive products (Figure 5C).

Peak ii is supposed to have the following structures on the basis of its conversion to a fucosylated trimannosyl core by digestion with jack bean β-*N*-acetylhexosaminidase (Figure 4D, solid line) and methylation data (Table I):

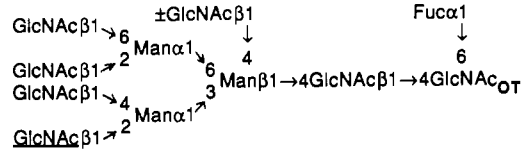

These structures are supported by the following evidence. By the first and the second cycles of Smith degradation, peak ii was sequentially converted to the same radioactive products as those produced from peak i (Figure 5A,B), respectively. These results indicate that the GlcNAcβ1→4(GlcNAcβ1→2)Manα1→ group in peak ii is linked at the C-3 position of the β-mannosyl residue of fucosylated trimannosyl core. Diplococcal β-*N*-acetylhexosaminidase should remove the *N*-acetylglucosaminyl residue underlined in the proposed structure for peak ii according to its substrate specificity (Yamashita et al., 1981), and only one *N*-acetylglucosamine residue was expectedly removed from peak ii by this enzyme digestion (Figure 5D).

Table II: Proposed Structures of Neutral Oligosaccharides in Aminopeptidase N[a]

Structures	Molar ratio (%) R*1	Molar ratio (%) R'*2
RCA⁻ (86%)		
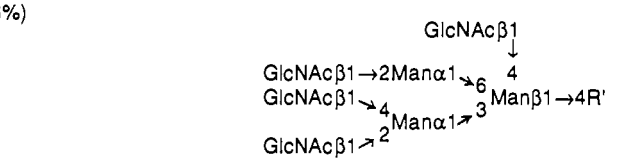	—	8 (*h*)
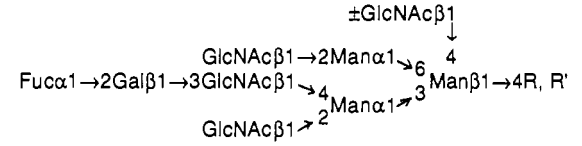	18 (*a*)*3	15 (*i*)
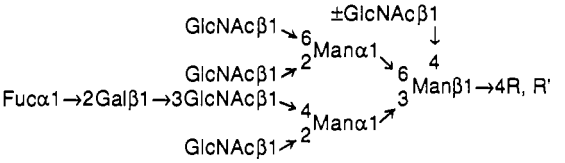	14 (*b*)	13 (*j*)
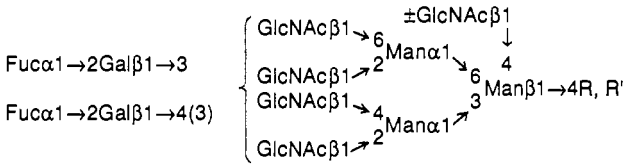	11 (*c*)	3 (*k*)
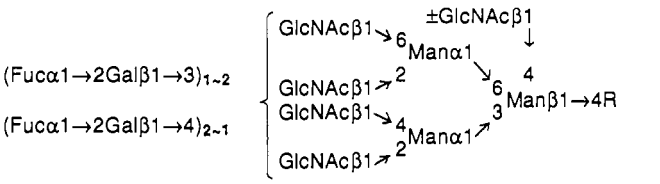	4 (d)	
RCA^r (7%)		
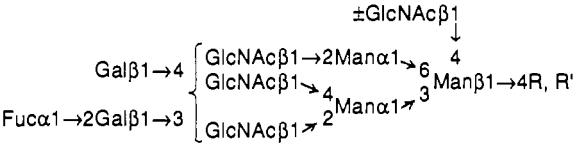	1.4 (*e*)	1.2 (*l*)
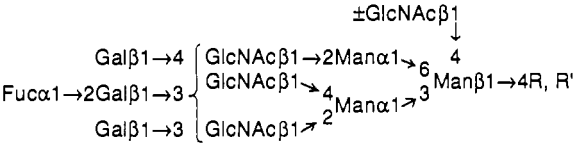	1.6 (*f*)	0.8 (*m*)
	2 (*g*)	
Con A⁺ (7%)		
high mannose-type	—	7 (*n*)

[a] Asterisked numbers indicate (*1) R = GlcNAcβ1→4(Fucα1→6)GlcNAc, (*2) R′ = GlcNAcβ1→4GlcNAc, and (*3) components in Figure 3.

That the Fucα1→2Gal groups are linked to *N*-acetylglucosamine residues in both peaks i and ii are determined as follows. The defucosylated components a–d were first digested with jack bean β-*N*-acetylhexosaminidase to remove terminal *N*-acetylglucosamine residues and then were digested with jack bean β-galactosidase. The resulting radioactive products from components a, b, c, and d were converted to the fucosylated trimannosyl core by jack bean β-*N*-acetylhexosaminidase digestion with release of one, one, two, and three *N*-acetylglucosamine residues exposed after degalactosylation, respectively (data not shown). Methylation data of peaks i and ii showed the decrease of 3,6-di-*O*-methyl-2-(*N*-methylacetamido)-2-deoxyglucitol and the complete absence of 4,6-di-*O*-methyl-2-(*N*-methylacetamido)-2-deoxyglucitol, which were

detected prior to degalactosylation, with the increase of 3,4,6-tri-*O*-methyl-2-(*N*-methylacetamido)-2-deoxyglucitol (Table I). These data indicate that either or both of the Fucα1→2Galβ1→3GlcNAc and Fucα1→2Galβ1→4GlcNAc groups are included in components a, b, c, and d. To discriminate these two galactosyl linkages, we used diplococcal β-galactosidase, which is well-known to cleave the Galβ1→4GlcNAc linkage but not the Galβ1→3GlcNAc linkage (Paulson et al., 1978). When the defucosylated components a and b were incubated with this enzyme under the condition that Galβ1→4GlcNAc linkages in complex-type oligosaccharides are easily cleaved, there was no release of galactose residue. Thus, it is reasonable to propose that a galactosyl residue in each of components a and b is attached to an *N*-acetylglucosamine residue by β1→3 linkage. On the other hand, one of the two galactose residues was removed from 77% of the defucosylated component c and no galactose residue was removed from the remainder by diplococcal β-galactosidase digestion, indicating that component c is composed of an oligosaccharide with one each of the Fucα1→2Galβ1→4GlcNAc and the Fucα1→2Galβ1→3GlcNAc groups and an oligosaccharide with two Fucα1→2Galβ1→3GlcNAc groups. By the same digestion, one of the three galactose residues was also removed from 20% of the defucosylated component d and two were removed from the remainder, respectively. The result indicates that component d is a mixture of oligosaccharides, one of which contains one Fucα1→2Galβ1→4GlcNAc and two Fucα1→2Galβ1→3GlcNAc groups and another of which contains two Fucα1→2Galβ1→4GlcNAc and one Fucα1→2Galβ1→3GlcNAc groups.

On the basis of these results and additional data described below, the structures of components a, b, c, and d in the AAL^+RCA^- fraction are proposed as shown in Table II. That bisecting *N*-acetylglucosamine residues are not galactosylated is based on the fact that 2-mono-*O*-methylmannitol disappeared with an increase of 2,4-di-*O*-methylmannitol after digestion of the defucosylated AAL^+RCA^- fraction with jack bean β-*N*-acetylhexosaminidase (data not shown). The location of one Fucα1→2Galβ1→3GlcNAc group in each of components a and b was determined by the following experiments. The defucosylated components a and b were digested with jack bean β-*N*-acetylhexosaminidase to remove all the terminal *N*-acetylglucosamine residues and then with jack bean β-galactosidase. As expected, this digestion gave a radioactive product from each of them with the same elution position as GlcNAc·Man_3·GlcNAc·Fuc·$GlcNAc_{OT}$. Possible structures for the product (A) from component a and that (B) from component b are considered to be as follows:

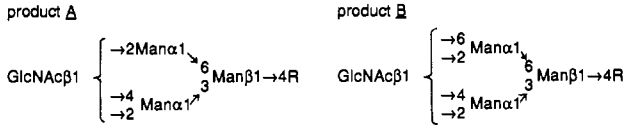

in which R represents GlcNAcβ1→4(Fucα1→6)$GlcNAc_{OT}$. An α-mannosyl residue was released from product A and also from product B by jack bean α-mannosidase, but it was not released by *A. saitoi* α-mannosidase II. Since α-mannosidase II is known to cleave the Manα1→3Man linkage in products A and B but not the Manα1→6Man linkage (Amano & Kobata, 1986), it is suggested that the *N*-acetylglucosamine residue should be linked to the Manα1→3 residue by β1→2 or β1→4 linkage. When both products A and B were incubated with diplococcal β-*N*-acetylhexosaminidase, which cleaves the GlcNAcβ1→2Man linkage but not the GlcNAcβ1→4Man linkage (Yamashita et al., 1981), there was no release of an *N*-acetylglucosamine residue. Thus, it is likely that the Fucα1→2Galβ1→3 group is linked to the GlcNAcβ1→4Manα1→3 arm of components a and b.

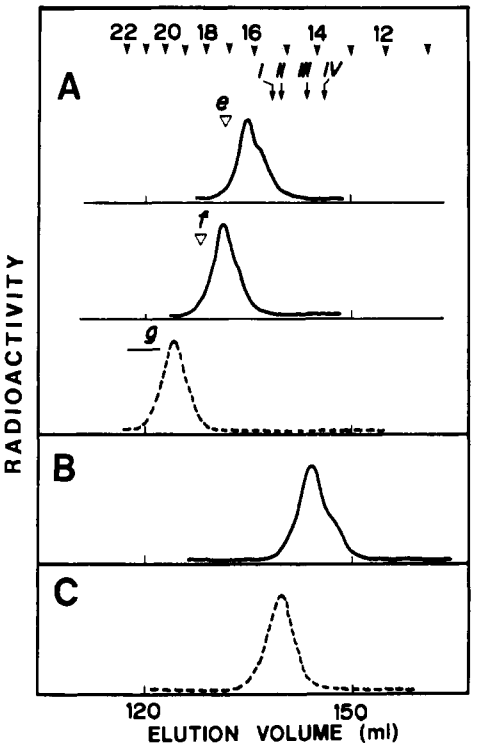

FIGURE 6: Sequential exoglycosidase digestion of components e, f, and g. The components e and f indicated by open triangles and the component g indicated by a bar were digested with *Corynebacterium* α-fucosidase (panel A). The defucosylated components e and f (solid lines in panel A) were digested with jack bean β-galactosidase to produce the same products (panel B). The defucosylated component g (dotted line in panel A) was digested with jack bean β-galactosidase (panel C). Arrows I, II, III, and IV are the same as in Figure 4, and black arrowheads are the same as in Figure 3.

Structural Analysis of Oligosaccharides in the AAL^+RCA^r Fraction. When digested with *Corynebacterium* α-fucosidase, one fucose residue was removed from each of the components e and f (solid lines in Figure 6A). By jack bean β-galactosidase digestion, the defucosylated components e and f were converted to the same radioactive product with the release of two and three galactose residues, respectively (Figure 6B). The elution position of the product was the same as that of peak i in Figure 4B, and their structural identity was confirmed in the same manner as that described for peak i (Figures 4D and 5A–C). These results indicate that both components e and f are triantennary oligosaccharides with different outer chain structures. When digested with jack bean β-galactosidase, one galactose residue was removed from component e and two residues were removed from component f. From these results, it is suggested that component e contains one each of the Galβ1→GlcNAc and Fucα1→2Galβ1→GlcNAc groups and a terminal *N*-acetylglucosamine residue in its outer chain moiety and that component f contains two Galβ1→GlcNAc groups and one Fucα1→2Galβ1→GlcNAc group. By diplococcal β-galactosidase digestion, only one galactose residue was removed from each of the components e and f before and after defucosylation (data not shown), indicating that one Galβ1→4GlcNAc group occurs in a non-fucosylated form in each of the components e and f, respectively. On the basis of these data, their structures are proposed as shown in Table II.

Component g, which was eluted from 20 to 22 glucose units (Figure 3B), was converted to a radioactive peak with 19.4 glucose units by *Corynebacterium* α-fucosidase digestion (dotted line in Figure 6A). From the difference between elution positions before and after the enzyme digestion, it was estimated that one to three fucose residues were released. When the defucosylated product was digested with jack bean β-galactosidase, four galactose residues were released (Figure 6C). That the peak in Figure 6C is the same as peak ii in Figure 4C was confirmed by the same manner as that described for peak ii. Thus, the data indicate that component g is a mixture of tetraantennary oligosaccharides with and without bisecting *N*-acetylglucosamine residues and that one to three of the four galactose residues included in this component occur as Fucα1→2Gal. Since diplococcal β-galactosidase digestion of the defucosylated component g produced three radioactive products in a molar ratio of 1:1:2 by releasing one, two, and three galactose residues, respectively (data not shown), it is concluded that the defucosylated component g is a mixture of oligosaccharides carrying the Galβ1→4GlcNAc group and the Galβ1→3GlcNAc group in molar ratios of 1:3, 2:2, and 3:1 in their outer chain moieties, respectively. On the basis of these data, the structures of oligosaccharides in component g are proposed as shown in Table II.

Structural Analysis of Oligosaccharides in the AAL⁻RCA⁻ and the AAL⁻RCA^r Fractions and the AAL⁻Con A⁺ Fraction. Components h, i, j, and k in the AAL⁻RCA⁻ fraction and components l and m in the AAL⁻RCA^r fraction were analyzed by a strategy similar to that used for those in the AAL⁺RCA⁻ and the AAL⁺RCA^r fractions, respectively. The results will be briefly described below. All the exoglycosidase digestions of components i, j, k, l, and m gave the same results as components a, b, c, e, and f, respectively, except for the shift of each radioactive peak to the smaller size by one glucose unit because of the absence of a fucose residue linked to the reducing terminal *N*-acetylglucosamine residue of trimannosyl core. Therefore, components i, j, k, l, and m are considered to be counterparts having non-fucosylated trimannosyl cores of components a, b, c, e, and f, respectively (Table II). Component h was converted to the non-fucosylated trimannosyl core by jack bean β-*N*-acetylhexosaminidase digestion with release of four *N*-acetylglucosamine residues (data not shown). Since this component was eluted at the same position as authentic bisected triantennary oligosaccharide, $GlcNAc_3$·Man_2·GlcNAc·Man·GlcNAc·$GlcNAc_{OT}$, and only one *N*-acetylglucosamine residue was expectedly removed by diplococcal β-*N*-acetylhexosaminidase digestion, its structure is proposed as shown in Table II. Triantennary structures of component h and defucosylated, degalactosylated component i were confirmed by methylation analysis and Smith degradation as in the case of peak i in Figure 4B. Tetraantennary structures of defucosylated, degalactosylated components i and k were also confirmed in the same manner as in the case of peak ii in Figure 4C.

Component m in the AAL⁻Con A⁺ fraction is supposed to be a mixture of high mannose type oligosaccharides on the basis of its behavior on the lectin column and its elution pattern from a Bio-Gel P-4 column. Therefore, the fraction was digested with *A. saitoi* α-mannosidase I, which cleaves specifically the Manα1→2Man linkage (Yamashita et al., 1980), and then analyzed by Bio-Gel P-4 column chromatography. A single radioactive peak with the same elution position as authentic Man_5·GlcNAc·$GlcNAc_{OT}$ was detected (data not shown). Sequential digestion of this component with jack bean α-mannosidase, β-mannosidase, and jack bean β-*N*-acetylhexosaminidase revealed that its structure was $(Man\alpha1\rightarrow)_4$-Manβ1→GlcNAcβ1→$GlcNAc_{OT}$ (data not shown). These results indicate that the AAL⁻Con A⁺ fraction contains a series of high mannose type oligosaccharides.

Discussion

In this study, we have elucidated the structures of neutral oligosaccharides that amount to 74% of the total N-linked sugar chains of rat small intestinal aminopeptidase N. The data indicate that the enzyme contains a variety of complex-type oligosaccharides with a small amount of high mannose type oligosaccharides. The complex-type oligosaccharides are composed of 2,4-branched triantennary and tetraantennary oligosaccharides with bisected and non-bisected trimannosyl cores. Several interesting structural characteristics are found in their outer chain moieties. First, most of the oligosaccharides are not completely galactosylated. The resulting oligosaccharides with exposed *N*-acetylglucosamine residues account for 89% of the total neutral oligosaccharides. Second, the galactose residues partly expressed in the outer chain moieties are extensively fucosylated by α1→2 linkage, resulting in the formation of H antigenic determinants of the ABO blood group system. A total of 85% of the neutral oligosaccharides express these determinants, while only 7% of the oligosaccharides bear exposed galactose residues. Third, these fucosylated and non-fucosylated galactose residues are linked to *N*-acetylglucosamine residues by β1→3 and β1→4 linkages. The Galβ1→3GlcNAc (type 1 chain) and the Galβ1→4GlcNAc group (type 2 chain) are included in 85% and 22% of the neutral oligosaccharides, respectively.

Some of these characteristics are regarded as the structural basis of the chromatographic behavior of this enzyme on immobilized lectin columns, which has previously been observed (Erickson & Kim, 1983). The low content of the high mannose type oligosaccharides explains the fact that only a small population of the enzyme bound to the Con A–Sepharose column. That most of the enzyme passed through the RCA-I–Sepharose column is also explained by the low expression of exposed galactose residues in the oligosaccharides, which results from not only the decreased galactosylation but also the extensive fucosylation of galactose residues. The enzyme in the proximal segment of the small intestine interacts to a lesser degree with the RCA-I–Sepharose column to than that in the distal segment. This has been observed not only in aminopeptidase N but also in other enzymes such as alkaline phosphatase, sucrase, and dipeptidylpeptidase IV (Morita et al., 1986). The present data suggest that these glycoenzymes are differently galactosylated and fucosylated depending on their proximal–distal location in the small intestine.

When the glycosylation pattern of rat intestinal aminopeptidase N is compared with those of rat renal brush-border membrane glycoenzymes, such as γ-glutamyltranspeptidase (Yamashita et al., 1983a), aminopeptidase N, and dipeptidylpeptidase IV (Yamashita et al., 1988), the following aspects become evident. All the enzymes are similar in that most of their N-linked oligosaccharides contain bisecting *N*-acetylglucosamine residues in their trimannosyl cores and exposed *N*-acetylglucosamine residues in their outer chain moieties. This similarity is of interest in view of the targeting of these enzymes to the apical side membranes of polarized epithelial cells. It will be important to investigate the sugar chains of glycoproteins in the basolateral side membranes in the future. Another aspect to be noted is the difference found between the intestinal enzyme and the kidney enzymes. The intestinal aminopeptidase N is quite unique in that the enzyme contains the type 1 chain and the type 1H and type 2H de-

terminants (Fucα1→2Galβ1→3 and 4GlcNAc) in the outer chain moieties of the oligosaccharides, which are not included in the three kidney enzymes at all. The H antigenic determinants have not been found in other rat glycoproteins such as serum α_1-acid glycoprotein (Yoshima et al., 1981), liver γ-glutamyltranspeptidase (Yamashita et al., 1983b), and erythrocyte membrane glycoproteins (Matsumoto et al., 1982a,b). Thus, the present data provide another example of the organ-specific difference in sugar chains as evidenced for the first time in γ-glutamyltranspeptidase in regard to the expression of bisecting *N*-acetylglucosamine residues (Yamashita et al., 1983c).

The present study indicates that the intestinal aminopeptidase N is enriched with neutral oligosaccharides in which high mannose type oligosaccharides are included to a quite small extent. It is also known that 80% of the N-linked sugar chains of rat small intestinal dipeptidylpeptidase IV are of neutral complex type (Erickson et al., 1983). In addition to these purified enzymes, rat small intestinal brush-border membranes have been shown to contain a low amount of sialic acid residues (Morita et al., 1986). Since the low expression of sialylated oligosaccharides as well as high mannose type oligosaccharides has been found in the glycopeptides of human small intestinal epithelial cells (Finne et al., 1989), these structural features seem to be common to the intestinal glycoproteins regardless of species. This is of particular interest in view of the interaction of host epithelial cells with some bacteria. It is well known that the adhesion of *Escherichia coli* and other Gram-negative bacteria to host epithelium is mediated by bacterial fimbriae (Beachey, 1981). Most *E. coli* strains contain type 1 fimbriae, which bind to α-mannosyl residues (Ofek et al., 1977). K99 Fimbriae produced by enterotoxigenic *E. coli*, which causes diarrhea in some animals up to a few weeks after birth (Runnels et al., 1980), and S fimbraie of *E. coli* with serotype O18:H1:H7, which causes meningitis and septicemia in newborn infants (Korhonen et al., 1985), have been shown to recognize sialic acid residues (Lindahl et al., 1987; Parkkinen et al., 1986). Therefore, the low expression of sialic acids and terminal α-mannosyl residues in the intestinal glycoproteins seems to be important in regard to the host defense against pathogenic bacteria. From the analysis of the sialic acid and fucose content and the lectin binding to the membranes, the decreased sialylation has been shown to occur with the increased fucosylation in the brush-border membrane glycoconjugates of rat small intestine during postnatal development (Torres-Pinedo & Mahmood, 1984). This change is reasonable in the respect that infection of host animals with the enterotoxigenic *E. coli* described above is restricted to the early stages after birth. Accordingly, it is suggested that the expression of H antigenic determinants as demonstrated in aminopeptidase N of adult rats may regulate the susceptibility of the host animals to bacterial infection by excluding terminal sialylation of the intestinal glycoconjugates.

Acknowledgments

We express our gratitude to Ms. Yumiko Kimizuka for her skillful secretarial assistance.

References

Amano, J., & Kobata, A. (1986) *J. Biochem.* (*Tokyo*) *99*, 1645–1654.

Beachey, E. H. (1981) *J. Infect. Dis. 143*, 325–345.

Erickson, R. H., & Kim, Y. S. (1983) *Biochim. Biophys. Acta 743*, 37–42.

Erickson, R. H., Bella, A. M., Jr., Brophy, E. J., Kobata, A., & Kim, Y. S. (1983) *Biochim. Biophys. Acta 765*, 258–265.

Finne, J. (1986) *Infect. Immun. 54*, 37–42.

Finne, J., Breimer, M. E., Hansson, G. C., Karlson, K. A., Leffler, H., Vliegenthart, J. F. G., & van Halbeek, H. (1989) *J. Biol. Chem. 264*, 5720–5735.

Grasgow, L. R., Paulson, J. C., & Hill, R. L. (1977) *J. Biol. Chem. 252*, 8615–8623.

Ichishima, E., Arai, M., Shigematsu, H., Kumagai, H., & Sumida-Tanaka, R. (1981) *Biochim. Biophys. Acta 658*, 45–53.

Kagawa, Y., Takasaki, S., Utsumi, J., Hosoi, K., Shimizu, H., Kochibe, N., & Kobata, A. (1988) *J. Biol. Chem. 263*, 17508–17515.

Kim, Y. S., & Brophy, E. J. (1976) *J. Biol. Chem. 251*, 3199–3205.

Korhonen, T. K., Valtonen, M. V., Parkkinen, J., Väisänen-Rhen, V., Finne, J., Dnorskov, F., Dnorskov, I., Svensson, S. B., & Mäkelä, P. H. (1985) *Infect. Immun. 48*, 486–491.

Kornfeld, K., Reitman, M. L., & Kornfeld, R. (1981) *J. Biol. Chem. 256*, 6633–6640.

Li, Y.-T., & Li, S.-C. (1972) *Methods Enzymol. 28*, 702–713.

Lindahl, M., Brossmer, R., & Waldström, T. (1987) *Glycoconjugate J. 4*, 51–58.

Matsumoto, A., Yoshima, H., Maeda, S., Shiraishi, N., & Kobata, A. (1982a) *Arch. Biochem. Biophys. 217*, 682–695.

Matsumoto, A., Yoshima, H., Shiraishi, N., Maeda, S., & Kobata, A. (1982b) *Arch. Biochem. Biophys. 217*, 696–709.

Morita, A., Miura, S., Erickson, R. H., Sleisenger, M. H., & Kim, Y. S. (1986) *Biochim. Biophys. Acta 883*, 506–516.

Ofek, I., Mirelman, D., & Sharon, N. (1977) *Nature* (*London*) *265*, 623–625.

Ogata, S., Muramatsu, T., & Kobata, A. (1975) *J. Biochem.* (*Tokyo*) *78*, 687–696.

Paulson, J. C., Prieels, J.-P., Grasgow, L. R., & Hill, R. L. (1978) *J. Biol. Chem. 253*, 5617–5624.

Runnels, P. L., Moon, H. W., & Schneider, R. A. (1980) *Infect. Immun. 28*, 298–300.

Takasaki, S., & Kobata, A. (1986) *Biochemistry 25*, 5709–5715.

Takasaki, S., Mizuochi, T., & Kobata, A. (1982) *Methods Enzymol. 83*, 263–268.

Takasaki, S., Murray, G. J., Furbish, F. S., Brady, R. O., Barranger, J. A., & Kobata, A. (1984) *J. Biol. Chem. 259*, 10112–10117.

Takeuchi, M., Takasaki, S., Miyazaki, H., Kato, T., Hoshi, S., Kochibe, N., & Kobata, A. (1988) *J. Biol. Chem. 263*, 3657–3663.

Torres-Pinedo, R., & Mahmood, A. (1984) *Biochem. Biophys. Res. Commun. 125*, 546–553.

Yamashita, K., Ichishima, E., Arai, M., & Kobata, A. (1980) *Biochem. Biophys. Res. Commun. 96*, 1335–1342.

Yamashita, K., Ohkura, T., Yoshima, H., & Kobata, A. (1981) *Biochem. Biophys. Res. Commun. 100*, 226–232.

Yamashita, K., Mizuochi, T., & Kobata, A. (1982) *Methods Enzymol. 83*, 105–126.

Yamashita, K., Hitoi, A., Matsuda, Y., Tsuji, A., Katunuma, N., & Kobata, A. (1983a) *J. Biol. Chem. 258*, 1098–1107.

Yamashita, K., HItoi, A., Taniguchi, N., Yokosawa, N., Tsukada, Y., & Kobata, A. (1983b) *Cancer Res. 43*, 5059–5063.

Yamashita, K., Hitoi, A., Tateishi, N., Higashi, T., Sakamoto, Y., & Kobata, A. (1983c) *Arch. Biochem. Biophys. 225*, 993–996.

Yamashita, K., Tachibana, Y., Shichi, H., & Kobata, A. (1983d) *J. Biochem.* (*Tokyo*) *93*, 135–147.

Yamashita, K., Kochibe, N., Ohkura, T., Ueda, I., & Kobata,

A. (1985) J. Biol. Chem. 260, 4688-4693.
Yamashita, K., Tachibana, Y., Matsuda, Y., Katsunuma, N., Kochibe, N., & Kobata, A. (1988) Biochemistry 27, 5565-5573.
Yoshima, H., Takasaki, S., & Kobata, A. (1980) J. Biol. Chem. 225, 10793-10804.
Yoshima, H., Matsumoto, A., Mizuochi, T., Kawasaki, T., & Kobata, A. (1981) J. Biol. Chem. 256, 8476-8484.

Study of Q_B^- Stabilization in Herbicide-Resistant Mutants from the Purple Bacterium *Rhodopseudomonas viridis*

Laura Baciou,‡ Irmgard Sinning,§ and Pierre Sebban*,‡

UPR 407, Bat 24 CNRS, Centres Réactionnels Photosynthétiques, Gif Sur Yvette 91198, France, and Max-Planck-Institut für Biophysik, Heinrich-Hoffmann Strasse 7, D-6000 Frankfurt 71, Germany

Received November 29, 1990; Revised Manuscript Received June 27, 1991

ABSTRACT: The pH dependences of the rate constants of $P^+Q_B^-$ (k_{BP}) and $P^+Q_A^-$ (k_{AP}) charge recombination decays have been studied by flash-induced absorbance change technique, in chromatophores of three herbicide-resistant mutants from *Rhodopseudomonas* (*Rps.*) *viridis*, and compared to the wild type. P, Q_A, and Q_B are the primary electron donor and the primary and the secondary quinone acceptors, respectively. The triazine resistant mutants T1 (Arg L217 → His and Ser L223 → Ala), T3 (Phe L216 → Ser and Val M263 → Phe), and T4 (Tyr L222 → Phe), all mutated in the Q_B binding pocket of the reaction center, have previously been characterized (Sinning, I., Michel, H., Mathis, P., & Rutherford, A. W. (1989) *Biochemistry 28*, 5544-5553). The pH dependence curves of k_{BP} in T4 and the wild type are very close. This confirms that the sensitivity toward DCMU of T4 is mainly due to a structural rearrangement in the Q_B pocket rather than to a change in the charge distribution in this part of the protein. In T3, a 6-fold increase of k_{AP} is observed (k_{AP} = 4200 ± 300 s^{-1} at pH 8) compared to that of the wild type (k_{AP} = 720 ± 50 s^{-1} at pH 8). We propose that the Val M263 → Phe mutation induces a free energy decrease between $P^+Q_A^-$ and P^+I^- ($\Delta G°_{IA}$) (I is the primary electron acceptor) of about 49 meV. The very different pH dependence of k_{AP} in T3 suggests a substantial change in the Q_A pocket. The 2.5 times increase of k_{AP} above pH 9.5 in the wild type is no longer detected in T3. Instead, a decrease of k_{AP} is observed above pH 9.5 (k_{AP} = 5100 ± 300 s^{-1} at pH 9.5 and k_{AP} = 3700 ± 300 s^{-1} at pH 11). Since in *Rps. viridis* the k_{AP} variations reflect the changes of $\Delta G°_{IA}$, it seems that the protonatable groups(s) involved in the increase of k_{AP} in the wild type above pH 9.5 has shifted closer to I^- than to Q_A^- in T3. The pH dependence of k_{BP} in T3 is also very different from that of the wild type. The 6-fold increase observed in the wild type in the pH range 5.5-8 is no longer detected in T3. We suggest that the Phe L216 → Ser mutation has an overall effect of shifting to lower pH the pK of the group (pK ~ 6.5) involved in the $\Delta G°_{BA}$ (free energy difference between $P^+Q_B^-$ and $P^+Q_A^-$) variations at low pH in the wild type. The temperature dependences of k_{AP}, k_{BP}, and K_2, the $Q_A^-Q_B \leftrightarrow Q_AQ_B^-$ equilibrium constant, have been determined in T3 and the wild type. At pH 8, the energy barrier between Q_A^- and Q_B^- is substantially increased in T3 ($\Delta G°_{BA}$ = −0.224 ± 0.015 eV) compared to that of the wild type ($\Delta G°_{BA}$ = −0.131 + 0.015 eV). The relative contribution of enthalpic and entropic terms to $\Delta G°_{BA}$ is very different in T3 and the wild type. In T1, above pH 7, Q_B^- is destabilized compared to the wild type. Assuming that this effect is mainly due to the absence of the positive charge present on Arg L217, we suggest that the apparent pK of His L217 in T1 is 8.3 ± 0.2. The K_2 values in T1, T4, and wild type have been compared with the previously measured relative binding affinities of Q_B (Q_{50}'s). The Q_B binding pocket of the wild type looks well designed for a simultaneous optimization of K_2 and Q_{50}'s.

The absorption of light energy by photosynthetic organisms results in the creation of a transmembrane charge-separated state of the reaction centers, in less than a nanosecond. The photosynthetic reaction center from *Rhodopseudomonas* (*Rps.*) *viridis* is composed of four polypeptides, the so-called H, M, and L subunits and a tightly bound cytochrome *c*. The three-dimensional structure of the reaction centers from *Rps. viridis* and *Rhodobacter* (*Rb.*) *sphaeroides* became known since their successful crystallization and X-ray structure analysis (Allen et al., 1988; Arnoux et al., 1989; Chang et al., 1986; Deisenhofer et al., 1985). The primary charge separation occurs in these reaction centers between a dimer of bacteriochlorophyll, P, and a quinone, Q_A, bound to the M polypeptide. The electron present on Q_A is then transferred to a secondary quinone, Q_B (bound to the L polypeptide), which can be doubly reduced. Q_B^- is tightly bound to the reaction centers (Wraight, 1981), whereas Q_B^{2-} is loosely bound and is supposed to leave the reaction center in its quinol state, Q_BH_2, after two protons have been uptaken from the cytoplasm. In vivo, the redox potentials of the quinone molecules are very different compared to their values measured in different solvents (Gunner et al., 1986; Woodbury et al.,

* To whom correspondence should be addressed.
‡ Centres Réactionnels Photosynthétiques.
§ Max-Planck-Institut für Biophysik.

0006-2960/91/0430-9110$02.50/0